

## LATTICE DYNAMICS AND PHASE TRANSITIONS

# EPR Study of the Jahn–Teller Effect of $\text{Cu}^{2+}$ Ions in $\text{ZnGa}_2\text{O}_4$

A. M. Vorotynov\*, G. A. Petrakovskii, K. A. Sablina, A. F. Bovina, and A. D. Vasil'ev

*Kirensky Institute of Physics, Siberian Branch, Russian Academy of Sciences,  
Akademgorodok 50, Krasnoyarsk, 660036 Russia*

\* e-mail: sasa@iph.krasn.ru

Received March 30, 2010

**Abstract**—The Jahn–Teller effect in the  $\text{ZnGa}_2\text{O}_4$  spinel single crystal has been investigated using electron paramagnetic resonance of  $\text{Cu}^{2+}$  ions in the temperature range 110–560 K. It has been shown that copper ions occupy octahedral sites  $16d$  in the  $\text{ZnGa}_2\text{O}_4$  crystal with cubic symmetry  $O_h^7$  ( $Fd-3m$ ). At  $T < 560$  K, the octahedra undergo tetragonal distortions (predominantly tension) and rotation around the fourfold axes by the angle  $\theta \approx 2.6^\circ$ . The parameters of the spin Hamiltonian, which characterize the prolate ( $g_{\parallel} = 2.355$ ,  $g_{\perp} = 2.077$ ,  $A_{\parallel} = 116$  Oe,  $A_{\perp} = 12$  Oe) and oblate ( $g_{\parallel} = 2.018$ ,  $g_{\perp} = 2.246$ ,  $A_{\parallel} = 75$  Oe,  $A_{\perp} = 44$  Oe) octahedra, have been determined. At temperatures above 560 K, the static Jahn–Teller effect transforms into the dynamic effect and the spectrum of the magnetic resonance becomes isotropic with  $g = 2.116$  (the experimental frequency corresponds to the  $X$  band).

DOI: 10.1134/S1063783410110314

## 1. INTRODUCTION

Oxide spinels  $AB_2O_4$  with cations occupying the tetrahedral and octahedral sites in close cubic packing of oxygen anions belong to the most important and interesting oxides due to their wide application in sensors, various electron and microwave devices, and as catalysts [1, 2]. Recently, copper-based oxide spinels (copper ferrite) were suggested as a good catalyst for obtaining hydrogen from the oxidized hydrocarbons [3, 4]. The  $\text{CuFe}_2\text{O}_4$  ferrimagnetic spinel is of greatest interest in this class of compounds. The presence of the Jahn–Teller  $\text{Cu}^{2+}$  ions in its composition leads to interesting properties of this compound, for example, the structural phase transition from the tetragonal phase into the cubic phase upon varying the temperature. In addition, some diamagnetically diluted copper ferrites were investigated in [5–8]. It was suggested that the Jahn–Teller transition is the transition of the order–disorder type, but the exact nature of this transition still remains unclear.

It is known that the method of the magnetic resonance allows one to reveal local distortions of the crystal structure, coordination of magnetic ions, and their nonequivalent sites in the lattice. In order to investigate the distortions of the crystal structure during the Jahn–Teller transition in oxide spinels, it was necessary to obtain the isostructural diamagnetic analog of the copper ferrite of the composition  $\text{Zn}_{1-x}\text{Cu}_x\text{Ga}_2\text{O}_4$  ( $x < 0.05$ ), the concentration of copper ions in which would be sufficient for the observation of the single-ion magnetic resonance spectra. It was also necessary to investigate the temperature and orientation depen-

dences of the magnetic resonance spectra in order to determine the coordination and parameters of the spin Hamiltonian of copper ions in the crystal and the character of the Jahn–Teller distortions.

## 2. SAMPLE PREPARATION AND EXPERIMENTAL TECHNIQUE

The  $\text{Zn}_{1-x}\text{Cu}_x\text{Ga}_2\text{O}_4$  single crystals were grown by the solution–melt method. The eutectic  $\text{PbO}-\text{B}_2\text{O}_3$  mixture (88.2 wt %  $\text{PbO}$  and 11.8 wt %  $\text{B}_2\text{O}_3$ ) with the melting point of  $500^\circ\text{C}$  was used as the solvent. The molar ratio of  $\text{ZnO}$  and  $\text{Ga}_2\text{O}_3$  was 1 : 1. The ratio solvent/ $\text{ZnGa}_2\text{O}_4$  was 4 : 1. The  $\text{Zn}_{1-x}\text{Cu}_x\text{Ga}_2\text{O}_4$  single crystals with  $x = 0.05$  were grown in capped platinum crucibles at  $T_{\text{max}} = 1200^\circ\text{C}$  and a cooling rate of  $6^\circ\text{C}/\text{h}$  to  $900^\circ\text{C}$ . The solvent was removed from crystals via boiling in a 20% nitric acid solution.

The crystal structure of the samples was investigated by the X-ray diffraction for the powders obtained by grinding the grown single crystals. Space group  $O_h^7$  ( $Fd-3m$ ) with lattice constant  $a = 8.330 \text{ \AA}$  was determined. The crystals had linear sizes up to 2 mm and the shape of the regular octahedron. The arrangement of crystallographic axes with respect to crystal faces is shown in Fig. 1. The fourfold axes come out from the octahedron vertices, while the threefold axes are perpendicular to its faces.

A fragment of the crystal structure of the cubic  $\text{ZnGa}_2\text{O}_4$  is shown in Fig. 2. Copper ions can occupy two crystallographic sites, namely,  $8a$  (the tetrahedral

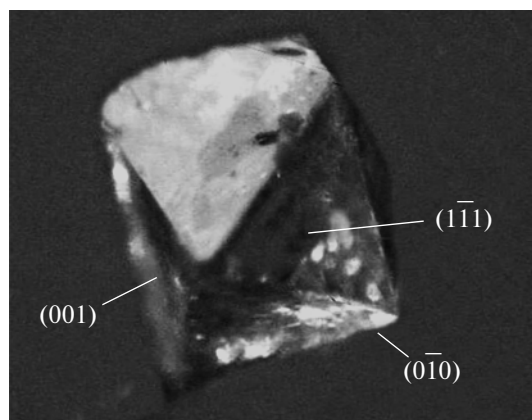


**Fig. 1.** Shape of the crystal and directions of the crystallographic axes connected to facing. The  $[001]$  and  $[0\bar{1}0]$  axes come from the vertices of the octahedron, and the  $[\bar{1}\bar{1}\bar{1}]$  axes are perpendicular to its faces.

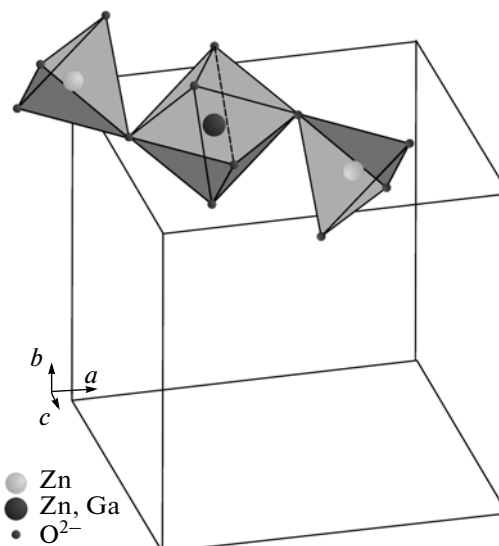


**Fig. 2.** A fragment of the crystal structure of  $\text{ZnGa}_2\text{O}_4$ .

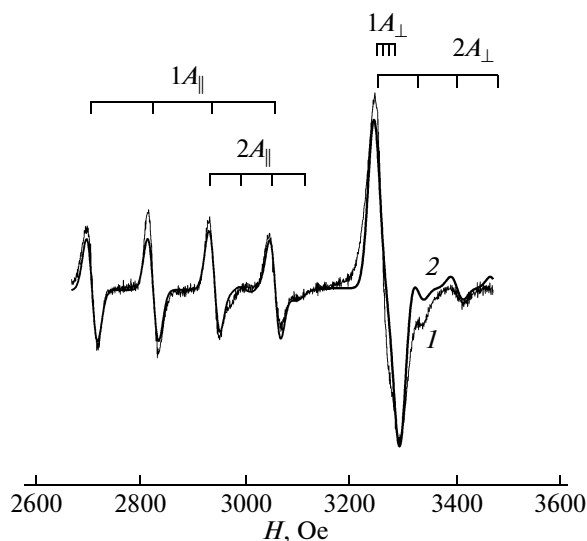


**Fig. 3.** Magnetic resonance spectrum with the orientation of the external magnetic field parallel to one of the  $C_4$  axes: (1) experiment and (2) theory (see text). Shown at the top are the positions of the resonant transitions for copper ions in sites 1 and 2.

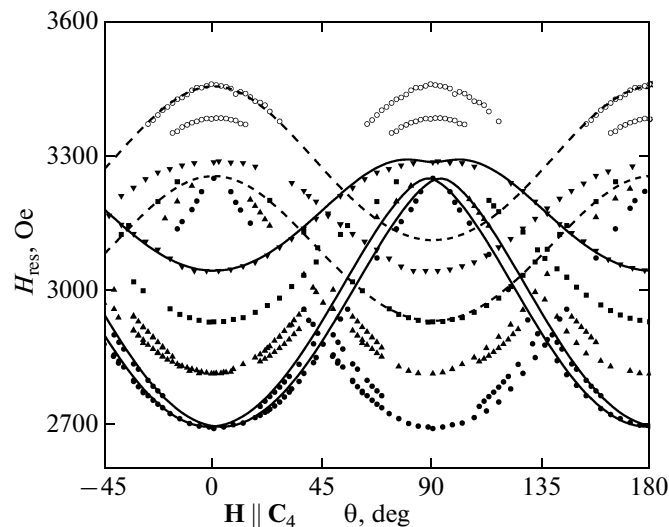


**Fig. 4.** Angular dependences of the magnetic resonance spectrum ( $\mathbf{H} \perp C_4$ ,  $T = 110$  K). Points are the experimental positions of the HFC lines, and the solid and dashed lines correspond to the theoretical curves for sites 1 and 2, respectively (see text).

environment of oxygen ions) and  $16d$  (the octahedral environment of oxygen ions).

The magnetic resonance was investigated on Bruker Elexsys E580 and Radiopan SE/X-2544 spectrometers operating in the  $X$  band in a temperature range of 80–560 K.

### 3. RESULTS AND DISCUSSION

The shape of the spectrum with the orientation of the magnetic field along one of  $C_4$  axes ( $T = 110$  K) is

shown in Fig. 3. The spectrum consists of four lines of almost identical intensity (the left part of the spectrum), an intense line in the field 3265 Oe, and weakly intense lines in the high-field part of the spectrum.

The angular dependence of the magnetic resonance spectrum with the orientation of the external magnetic field perpendicularly to one of the fourfold axes at 110 K is shown in Fig. 4 (Fig. 4 does not show the locations of resonant lines independent of the orientation and corresponding to the magnetic center, for which always  $\mathbf{H} \perp C_4$ ). As the external magnetic field

Parameters of the spin Hamiltonian (1) for Cu<sup>2+</sup> in ZnGa<sub>2</sub>O<sub>4</sub> at  $T = 110$  K

Site	$g_{\parallel}$	$A_{\parallel}$ , Oe	$g_{\perp}$	$A_{\perp}$ , Oe	$g_{av} = (g_{\parallel} + 2g_{\perp})/3$
1	2.355 <sup>1</sup>	116 <sup>1</sup>	–	–	2.170
	2.355 <sup>2</sup>	116 <sup>2</sup>	2.077 <sup>2</sup>	12 <sup>2</sup>	
2	2.018 <sup>1</sup>	75 <sup>1</sup>	–	–	2.170
	2.018 <sup>2</sup>	75 <sup>2</sup>	2.246 <sup>2</sup>	44 <sup>2</sup>	

<sup>1</sup> Experimental values.<sup>2</sup> The values obtained with the WINEPR SimFonia v.1.26 program (Fig. 3).

deviates from  $C_4$  axis, splitting of two low-field lines in the spectrum is observed (Fig. 4). The analysis of the obtained angular dependences allowed us to assume that two nonequivalent copper sites denoted by indices 1 and 2 in Fig. 3 are present in the sample. Both sites are characterized by three mutually perpendicular axes  $C_4$ . The ratio of intensities of sites 1 and 2 allows us to conclude that site 1 is preferentially populated by copper ions.

The magnetic resonance spectrum was theoretically described in the context of the uniaxial spin Hamiltonian

$$\mathcal{H} = g_{\parallel}\beta H_z S_z + g_{\perp}\beta(H_x S_x + H_y S_y) + A_{\parallel}I_z S_z + A_{\perp}(I_x S_x + I_y S_y), \quad (1)$$

where  $S$  is the spin of the electron of the Cu<sup>2+</sup> ion ( $=1/2$ ),  $I$  is the spin of the nucleus <sup>63</sup>Cu ( $=3/2$ ), and  $A$  is the hyperfine coupling (HFC) constant. To determine the parameters of the spin Hamiltonian (1) at  $\theta = 90^\circ$  (when the HFC lines in practice merge, Fig. 4), we used the WINEPR SimFonia v. 1.26 program. The obtained constants of the spin Hamiltonian are presented in the table. The theoretical angular dependences of the center of gravity of the spectra of sites 1 and 2 and two HFC components extreme for each site with the parameters of the spin Hamiltonian from the table are presented in Fig. 4. The model spectrum and the location of resonant transitions for copper ions in sites 1 and 2 are shown in Fig. 3.

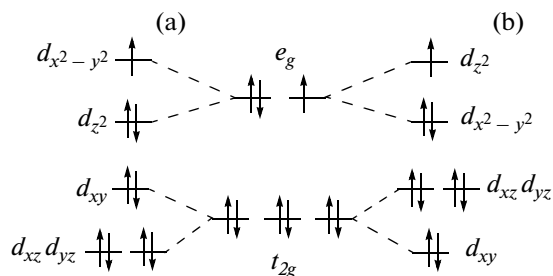


**Fig. 5.** Electron configuration of the Cu<sup>2+</sup> ion in the octahedral environment with a tetragonal distortion: (a) prolate octahedron and (b) oblate octahedron.

The obtained values of  $g$ -factors are typical of the Cu<sup>2+</sup> ions in the octahedral environment [9, 10]. In this case, the scheme of the energy levels for the Cu<sup>2+</sup> ion is shown in Fig. 5, and  $g$ -factors are determined by expressions [9, 11]  $g_{\parallel} = 2 - 8\lambda/\Delta$ ,  $g_{\perp} = 2 - 2\lambda/\Delta$  for site 1 of the prolate octahedron and  $g_{\parallel} = 2$ ,  $g_{\perp} = 2 - 6\lambda/\Delta$  for site 2 of the oblate octahedron, where  $\lambda$  is the constant of spin–orbit coupling and  $\Delta$  is splitting of levels  $t_{2g}$  and  $e_g$  in the cubic crystal field. Thus, we can identify the observed nonequivalent sites 1 and 2 as prolate and oblate along one of three mutually perpendicular  $C_4$  axes of the octahedron, respectively.

As it was already mentioned above, splitting of the resonant lines is observed for the resonant spectrum of the Cu<sup>2+</sup> ions in site 1, which is especially noticeable for first two low-field HFC components (Fig. 4). This fact indicates that the Jahn–Teller effect leads not only to the tetragonal distortion of the octahedral environment but also to the rotation of octahedra (at least in site 1) by angle  $\theta \approx 2.6^\circ$ .

The modification of the magnetic resonance spectrum upon increasing the temperature and arbitrary orientation of the external magnetic field is shown in Fig. 6.

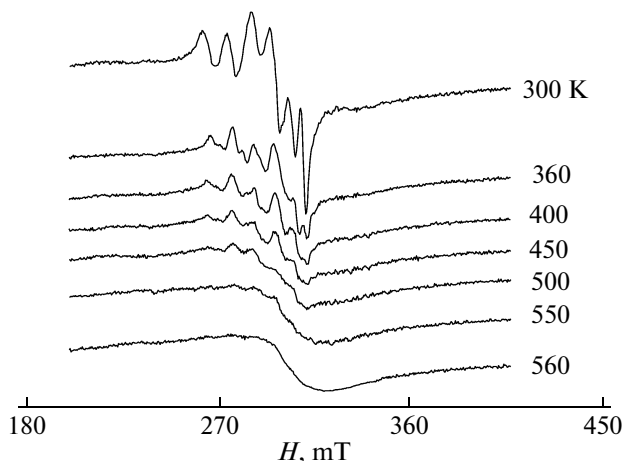


**Fig. 6.** Modification of the magnetic resonance spectrum with an increase in the temperature and an arbitrary orientation of the external magnetic field.

As the temperature increases, the HFC lines noticeably broaden, and at 560 K, the spectrum is the isotropic line with parameters  $g = 2.116$  and  $\Delta H = 373$  Oe. This is explained by the fact that at temperatures below 560 K, no transitions take place between the three vibrational levels of octahedra, which correspond to three equilibrium Jahn–Teller configurations (distortions along three fourfold axes) with a minimal energy. As the temperature increases, the thermal transitions from one equilibrium configuration into another one become possible (reorientation of distorted octahedron axes). If such transitions are highly probable, the dynamic Jahn–Teller effect is realized; if they proceed slowly, i.e., the system is frozen in one of the states, the static Jahn–Teller effect takes place. In the dynamic case, the deformations are averaged, and the pattern becomes spherically symmetric. In this case, a single line of the resonant absorption with  $g$ -factor  $g_{av} = (g_{\parallel} + 2g_{\perp})/3$  is observed. Let us note that the temperature of the transition from the static Jahn–Teller effect to the dynamic one, in our opinion, is rather close to the temperature of the structural phase transition in the  $\text{CuFe}_2\text{O}_4$  copper ferrite,  $T_c = 633$  K [12].

It should be noted that the distinction of the static and dynamic Jahn–Teller effects for the isolated centers is not of a principal value since one system with a characteristic transition time  $\tau \sim \hbar/\omega$  can manifest the characteristics of the dynamic Jahn–Teller effect in certain experiments, in which averaging over long time intervals is performed (for example, in NMR), while in other experiments, which are characterized by a short intrinsic time (for example, during the optical absorption), it can manifest the static Jahn–Teller effect.

#### 4. CONCLUSIONS

The performed investigations have shown that the copper ions are in octahedral sites  $16d$  of the  $\text{ZnGa}_2\text{O}_4$  cubic crystal. The magnetic resonance spectra are described by the spin Hamiltonian

$$\mathcal{H} = g_{\parallel}\beta H_z S_z + g_{\perp}\beta(H_x S_x + H_y S_y) + A_{\parallel}I_z S_z + A_{\perp}(I_x S_x + I_y S_y).$$

The Jahn–Teller effect is found, during which the tetragonal distortion (both tension and compression) of oxygen tetrahedra as well as their rotation by the angle  $\theta \approx 2.6^\circ$  take place. The parameters of the spin Hamiltonian at  $T = 110$  K are determined; they characterize the prolate ( $g_{\parallel} = 2.355$ ,  $g_{\perp} = 2.077$ ,  $A_{\parallel} = 116$  Oe, and  $A_{\perp} = 12$  Oe) and oblate ( $g_{\parallel} = 2.018$ ,  $g_{\perp} = 2.246$ ,  $A_{\parallel} = 75$  Oe, and  $A_{\perp} = 44$  Oe) octahedra. At temperatures above 560 K, the static Jahn–Teller effect transforms into the dynamic effect (the experimental frequency corresponds to the  $X$  band).

#### REFERENCES

1. A. Laobuthee, S. Wongkasemjit, E. Traversa, and R. M. Laine, *J. Eur. Ceram. Soc.* **20**, 91 (2000).
2. U. Luders, M. Bibes, K. Bouzehouane, E. Jacquet, J. P. Contour, S. Fusil, J. F. Bobo, J. Fontcuberta, A. Barthelemy, and A. Fert, *J. Appl. Phys.* **99**, 08K 301 (2006).
3. S. Kameoka, T. Tanabe, and A. P. Tsai, *Catal. Lett.* **100**, 89 (2005).
4. K. Faungnawakij, Y. Tanaka, N. Shimoda, T. Fukunaga, S. Kawashima, R. Kikuchi, and K. Eguchi, *Appl. Catal., A* **304**, 40 (2006).
5. R. K. Selvan, V. Krisham, Ch. O. Augustin, H. Bertagnolli, Ch. S. Kim, and A. Gedanken, *Chem. Mater.* **20**, 429 (2008).
6. X. X. Tang, A. Manthiram, and J. B. Goodenough, *J. Solid State Chem.* **79**, 250 (1989).
7. C. Villette, Ph. Tailhades, and A. Rousset, *J. Solid State Chem.* **117**, 64 (1995).
8. N. S. Gajbhiye, G. Balaji, S. Bhattacharyya, and M. Ghafari, *Hyperfine Interact.* **57**, 156 (2004).
9. A. Abragam and B. Bleaney, *Electron Paramagnetic Resonance of Transitions Ions* (Clarendon, Oxford, 1970; Mir, Moscow, 1972).
10. S.A. Al'tshuler and B. M. Kozyrev, *Electron Paramagnetic Resonance* (Nauka, Moscow, 1972; Academic, New York, 1964).
11. J. Wertz and J. Bolton, *Electron Spin Resonance* (McGraw-Hill, New York, 1972; Mir, Moscow, 1975).
12. K. I. Kugel' and D. I. Khomskii, *Usp. Fiz. Nauk* **136** (4), 621 (1982) [*Sov. Phys.—Usp.* **25** (4), 231 (1982)].

Translated by N. Korovin